

Coupled Cluster Calculation of the $n \rightarrow \pi^*$ Electronic Transition of Acetone in Aqueous Solution

Kestutis Aidias,[†] Jacob Kongsted,^{*} Anders Osted,[‡] and Kurt V. Mikkelsen[§]

Department of Chemistry, H. C. Ørsted Institute, University of Copenhagen, Universitetsparken 5, DK-2100 Copenhagen Ø, Denmark

Ove Christiansen^{||}

Department of Chemistry, University of Aarhus, Langelandsgade 140, DK-8000 Aarhus C, Denmark

Received: May 23, 2005; In Final Form: July 1, 2005

The combined linear response coupled cluster/molecular mechanics (CC/MM) scheme including mutual polarization effects in the coupling Hamiltonian is applied together with supermolecular CC methods to the study of the gas-to-aqueous solution blue shift of the $n \rightarrow \pi^*$ excitation energy in acetone. The aug-cc-pVDZ basis set is found to be adequate for the calculation of this excitation energy. In the condensed phase, the shift in the excitation energy is obtained by statistical averaging over 800 solute–solvent configurations extracted from a molecular dynamics simulation. We find the shift to be around 1100–1200 cm^{-1} depending on the specific model used to describe solvent polarization. The importance of including explicit polarization in both the molecular dynamics simulation as well as the CC/MM calculations is emphasized. Furthermore, the significant dependence of the excitation energy on the CO bond length of acetone is discussed.

I. Introduction

Modern electronic ab initio methods have undergone significant development during the past decades and are today sufficiently powerful to predict structures, energies, and various molecular properties of isolated small molecules with desired accuracy. However, the majority of experiments related to spectroscopic data are carried out in liquids or solutions. Thereby, a direct comparison between measured and calculated properties is difficult, since the neighboring molecules naturally perturb the molecular system in question. Consequently, different molecular properties may change because of intermolecular interactions, and some of them change very drastically. Moreover, some molecular processes such as charge transfer may be governed by the surrounding medium. Hence, the relevance of having a precise description of solvent effects is obvious.

Certainly, one could consider the molecular system large enough to capture relevant solvent effects and perform the needed high-level ab initio calculations. Unfortunately, these so-called supermolecule calculations are computationally very expensive, although low scaling electronic structure methods or semiempirical models can be very useful for this purpose. A considerable reduction in the number of solvent molecules included in the calculation may lead to inaccurate prediction of solvent effects, since a few molecules from the first solvation shell obviously cannot represent the whole solvent. Another approach coming to light with the early works of Onsager and

Kirkwood¹ is to replace the explicit solvent molecules with a homogeneous dielectric medium. According to this so-called dielectric continuum (DC) model,² the actual system is housed in a cavity within the dielectric medium. There are various modifications of the dielectric continuum model, and it has been applied to numerous problems. However, these models are not able to capture specific intermolecular interactions such as, for example, hydrogen bonds. Moreover, they have intrinsic parameters such as cavity size and shape, which are not determined theoretically and should, in general, be recalibrated for every individual method. Both supermolecule and dielectric continuum patterns do not regard the dynamical character of the liquid. The latter can be taken into account by, for example, molecular dynamics (MD) or Monte Carlo (MC) simulation methods.³ Also, Car–Parrinello MD (CPMD) simulations may be introduced.⁴

A very useful procedure to calculate molecular properties of molecules in liquids or solutions is based on simulation methods, where a sufficient number of configurations of the molecular ensemble are generated, and certain molecular properties are calculated at the desired level and finally averaged over all the configurations. The solute molecule is treated quantum mechanically (QM), while the solvent molecules can be described in terms of molecular mechanics (MM), resulting in combined quantum mechanics/molecular mechanics (QM/MM) methods.^{5–8} QM/MM methods can be refined by the inclusion of a dielectric continuum for description of the bulk structure.^{9,10} Pioneering studies of solvent effects on excitation energies using the QM/MM scheme including both explicit polarization effects and statistical averaging are due to Warshel et al.^{11,12} Later contributions have been reported by Gao et al.,¹³ Thompson et al.,^{5,14} and Warshel et al.¹⁵

Recently, we proposed a QM/MM method where the solute molecule is treated using coupled cluster (CC) electronic

^{*} To whom all correspondence should be addressed. Electronic mail: kongsted@chem.au.dk. Present address: Department of Chemistry, University of Aarhus, Langelandsgade 140, DK-8000 Aarhus C, Denmark.

[†] kestutis.aidias@ff.vu.lt. Permanent address: Faculty of Physics, Vilnius University, Sauletekio al. 9, LT-10222 Vilnius, Lithuania.

[‡] osted@theory.ki.ku.dk.

[§] kmi@theory.ki.ku.dk.

^{||} ove@chem.au.dk.

structure theory (the CC/MM model) and where the effect of explicit solvent polarization is accounted for in the optimization of the wave function.¹⁶ This method has, for example, been applied to the study of linear and higher-order response properties.^{17–19} Very recently, this model was successfully applied to the study of the vertical electronic excitation energy for the $n \rightarrow \pi^*$ electronic transition in formaldehyde solvated by water.²⁰

Stimulated by our previous success, here we apply the CC/MM scheme to the study of the vertical $n \rightarrow \pi^*$ electronic transition of acetone in aqueous solution. In the $n \rightarrow \pi^*$ electronic transition in acetone, an electron from the oxygen nonbonding lone pairs is promoted to the antibonding π^* orbital, leading to a reduction of the excited-state dipole moment as compared to that of the ground state. Consequently, in polar solvents, the solute is more favorably solvated in the electronic ground state than in the excited state. This results in a blue shift of the excitation energy of acetone in solution, as compared to the gas phase. In the cases of polar solutes and polar solvents, the electrostatic interactions are predominant, and the effects of dispersion and short-range repulsion may be modeled using an energy expression independent of the electronic degrees of freedom, i.e., dispersion and short-range repulsion do not contribute to the calculated molecular properties of the solute. However, in the case of apolar solvents, the effects of dispersion become very significant and should be properly considered to reproduce the reliable shift in excitation energy.²¹ The effect of magnetic interactions is usually small in magnitude and is thereby rarely necessary to take into consideration when investigating electronic excitations.

The experimental result for the $n \rightarrow \pi^*$ electronic excitation energy of acetone in a vacuum is $\sim 36\,200\text{ cm}^{-1}$ (4.488 eV), and the corresponding result in aqueous solution is $\sim 37\,760\text{ cm}^{-1}$ (4.682 eV), leading to a shift of around 1500–1600 cm^{-1} .^{22–24} The shift in the excitation energy of acetone in aqueous solution is a good benchmark for the theoretical solvation models, and in contrast to, for example, formaldehyde in aqueous solution, reliable experimental data do exist. Therefore, this system has been studied by various explicit and implicit solvation models such as the supermolecule approach,²⁵ reference interaction site self-consistent field (RISM-SCF),²⁶ dielectric continuum model,^{27,28} CPMD,^{29–32} and MD³³ or MC^{21,34–36} simulations with following QM/MM or supermolecule calculations possibly with included DC. In this paper, we consider the problem using CC/MM methods. To the best of our knowledge, this will be the first attempt to consider this problem by CC electronic structure theory, which in recent years has proven to be the most accurate *ab initio* method. CC calculations on acetone in a vacuum have previously been reported.³⁷

This paper has the following structure. In section II, we introduce the description of the method and computational details. Section III contains the discussion of basis set analysis and microsolvated results, together with MD simulation and the outcome of the CC/MM calculation. Finally, the summary in section IV finalizes this paper.

II. Method

For the calculation of the $n \rightarrow \pi^*$ electronic excitation energy of acetone in a vacuum and in aqueous solution, we use linear response coupled cluster (LRCC) theory.^{17,38} LRCC provides vertical electronic excitation energies based on knowledge of only the ground-state wave function. For the condensed-phase problem, we use an effective model in order to introduce the

solvent molecules. This effective model belongs to the class of combined quantum mechanics/molecular mechanics approaches and is denoted the combined coupled cluster/molecular mechanics (CC/MM) model.^{16,17,39} In the CC/MM model, the solute molecule is treated using coupled cluster electronic structure theory, while the solvent is described classically. Thus, we assign to each water molecule a set of atomic partial-point charges together with a set of van der Waals parameters. Here, the latter is described using a 6-12-type Lennard-Jones (LJ) potential. Polarization of the solvent by the solute may be treated at different levels of theory. In the simplest case, the partial charges simply have an enhanced magnitude (as compared to the vacuum charges), and polarization is thereby included implicitly. The CC/MM model also has the capability of including polarization explicitly, i.e., a dipole polarizability is assigned to each water molecule. This in combination with coupled cluster theory is a unique feature. The dipole polarizability gives rise to induced dipole moments which are introduced into the coupling between the two subsystems. The latter of the two approaches for introducing polarization effects increases the computational time considerably, but is usually very important for an accurate prediction of certain molecular properties of molecules in condensed phases.^{17–20}

One of the great advantages of using response theory^{38,40} to calculate the vertical electronic excitation energy is that only the ground state of the system has to be considered explicitly. Thus, we only need parameters for the ground state (and we only need to perform simulations of acetone in the ground state) in order to get information concerning the excitation processes. This is highly attractive, since one of the more difficult problems in molecular simulations is to get reliable results for especially the LJ parameters for excited states. Since the solvent reorganization time scale is much larger than the time scale for electronic processes, the use of response theory with ground-state MM parameters enables a physically correct picture of the excitation process, i.e., the solute is in equilibrium with the solvent but *only* for the ground state and *not* for the particular electronic excited state. Along this line, we note that models in which the electronic excitation energy is calculated on the basis of simulations of both the ground and excited states (using excited-state partial charges for the latter) actually assumes equilibrium between the solute and the solvent in both the ground and excited states, thereby describing a different situation. If, for example, solvent effects on the fluorescence from excited states is to be considered, such considerations are relevant, as is also the geometrical relaxation of the excited-state solute molecule.

With the linear response functions, a variety of molecular properties may be derived. Here, we only consider the dipole moment in the excited state (together with the dipole moment in the ground state) and the electronic excitation energy together with the corresponding oscillator strength for the $n \rightarrow \pi^*$ electronic transition.

The CC/MM method has been implemented in the Dalton program package.⁴¹ Here, we employ the coupled cluster singles and doubles (CCSD)⁴² implementation. The structural input to the Dalton CC/MM calculations is based on configurations dumped in an MD simulation using the MOLSIM program.⁵⁴ Using the MidasCpp program package,⁴³ we impose periodic boundary conditions, and each configuration is translated/rotated so that the acetone molecule is placed in the xz plane with the oxygen atom in the origin and the C_2 axis aligned with the molecular z axis. Finally, a spherical cutoff radius (unique to the CC/MM calculations) is used.

TABLE 1: Electronic Excitation Energy (E_{ex} , eV) and Dipole Moment in the Ground and Excited States (μ_z , D) for Acetone Using the Vacuum B3LYP/atx Optimized Geometry Calculated for Different Basis Sets and CC Methods^a

method/basis set	no. of basis funcs.	E_{ex}	μ_z^{gs}	μ_z^{ex}
CCSD/datz	440	4.556	2.958	1.660
CCSD/atx	322	4.558	2.959	1.654
CCSD/tz	204	4.584	2.790	1.549
CCSD/dadz	206	4.542	2.909	1.634
CCSD/adz	146	4.550	2.921	1.623
CCSD/dz	86	4.580	2.550	1.440
CC3/adz	146	4.523		

^aIn all calculations, we freeze the four lowest canonical orbitals (all of 1s character) of oxygen and carbon.

TABLE 2: Structural Data of Acetone in Vacuum and in Aqueous Solution (in angstroms and degrees) as Obtained by Geometry Optimization (vacuum) and Averaging of Two Equivalent Optimized Liquid-Phase Acetone Structures (water) (see text for details)

	in vacuum	in water	exptl ^a
$r(\text{OC1})$	1.210	1.225	1.215
$r(\text{C1C2})$	1.514	1.501	1.515
$r(\text{C2H1})$	1.087	1.087	1.086
$r(\text{C2H2})$	1.092	1.092	
$\angle(\text{OC1C2})$	121.7	121.4	121.8
$\angle(\text{C1C2H1})$	110.1	111.2	110.3
$\angle(\text{C1C2H2})$	110.2	109.6	
$\angle(\text{OC1C2H1})$	0.0	0.0	0.0
$\angle(\text{OC1C2H2})$	121.2	121.6	

^a Gas-phase data taken from ref 68.

III. Results and Discussion

A. Basis Set Analysis. In Table 1, we present the $n \rightarrow \pi^*$ electronic excitation energy of acetone in a vacuum together with the results for the dipole moments in the ground (gs) and excited (ex) states for different basis sets. The molecular geometry is found from optimization at the B3LYP/aug-cc-pVTZ level of theory (see Table 2 for the geometrical results). In Table 1, we use the abbreviation (d)axz for the (d)-aug-cc-pVXZ basis sets.^{44,45} Also, in this table we have included the number of basis functions for each entry. Concerning the CCSD results, we observe a systematic decrease in the excitation energy within the sequence xz, axz, and daxz ($x = \text{d, t}$). Furthermore, within the sequences (dz, tz), (adz, atz), and (dadz, datz), we observe a small increase in the excitation energy. However, if the dz and tz results are excluded, the changes are rather small, and for the excitation energy, the adz is seen to give fairly converged results. The error in the adz excitation energy as compared to the datz calculation is only around 48 cm^{-1} . Also, the errors in the dipole moments in the adz calculation relative to the datz results are only around -0.037 D. Thus, in the following, we will exclusively use the adz basis set for acetone.

In Table 1, we have also included the CC3/adz⁴⁶ results for the excitation energy. Here, we find that the effect of triples excitations is to lower the excitation energy by 0.027 eV (218 cm^{-1}). It is likely that the CC3 results for the excitation energy in acetone *in water* also will be lowered, thereby leading to a (partial) cancellation of this error in the calculation of the shift. However, for the *absolute* value of the excitation energy, this error still persists both in a vacuum and in solution, and may actually represent one of the largest uncertainties in our predictions.

B. Discussion of the Microsolvated Results. As an initial investigation of solvent effects on the $n \rightarrow \pi^*$ electronic excitation, we consider acetone microsolvated by two water

molecules. Such a microsolvated approach to solvation is not optimal for several reasons. First, in the microsolvated case, we derive the solute–solvent configuration(s) using ab initio energy minimization techniques. However, in the true liquid, the solute–solvent structures do not necessarily represent energy minima, leading to the conclusion that solvent effects cannot be predicted very accurately using microsolvated approaches. Second, the important statistics underlying the nature of a liquid are not included using microsolvated approaches. It is of course possible to include different microsolvated structures and then average over the property in order to include the statistics. However, this approach may quickly become highly expensive (in terms of CPU time), and finally, the microsolvated approach does not include the important long-range electrostatic effects due to solvent molecules beyond the first solvent shell. This approximation may be overcome by including in addition to some explicit solvent molecules a dielectric continuum. However, by still using this rather elaborate approach (solute + explicit solvent molecules + dielectric continuum combined with statistical averaging), the true discrete nature of the outer solvent molecules are still neglected. In this work, the main reason for considering the microsolvated approaches is that, because of the very small number of explicit solvent molecules, it allows for a comparison between the effective and supermolecular approaches, thereby justifying the effective (CC/MM) model.

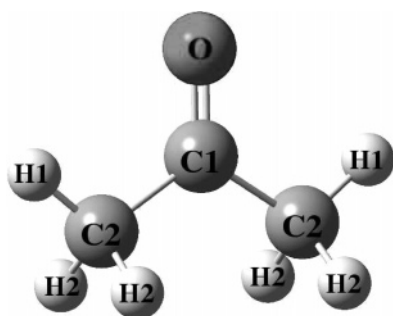
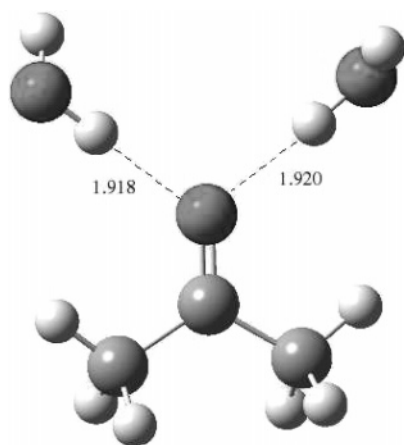
In Table 3, we show the results of the $n \rightarrow \pi^*$ electronic excitation in the system composed of acetone and two water molecules. The basis set used in the property calculations is the aug-cc-pVDZ basis set. The geometry of the supersystem has been found by geometry optimization (B3LYP/aug-cc-pVTZ/PCM) using the *Gaussian 03* program⁴⁷ and is shown in Figure 2. The vacuum reference (shown in Figure 1) has also been geometry-optimized using B3LYP/aug-cc-pVTZ. At the CCSD/adz level of theory, we have for the $n \rightarrow \pi^*$ electronic excitation energy a result of 4.746 eV, and the corresponding shift (including geometrical effects) is thereby 1581 cm^{-1} . Using instead the liquid structure for acetone as the reference, i.e., the structure for acetone found by optimizing acetone and two waters, we obtain an enhanced blue shift that amounts to 2323 cm^{-1} . Geometrical distortions are thereby found to affect the value of the shift considerably. Correcting in the latter calculation for basis set superposition errors (BSSE) has, as indicated in Table 3, essentially no effect.

Turning to the CC/MM predictions, we have in Table 3 included results using different descriptions for the water molecules. First, we describe the waters using the TIP3P⁴⁸ potential (see Table 4). This water potential describes polarization effects implicitly through enhanced values of the partial atomic charges. For the TIP3P potential, we obtain a shift in the $n \rightarrow \pi^*$ electronic excitation energy of 1863 cm^{-1} . This is 282 cm^{-1} (0.035 eV) higher than the corresponding supermolecular predictions. The rather large change in excitation energy in this case is due to the implicit description of polarization effects. This may be elaborated by including the polarization explicitly. The simple point-charge plus polarization (SPCpol)1 potential⁴⁹ (see Table 4) includes a dipole polarizability at the oxygen site and thereby accounts directly for many-body effects. Using this water potential, we obtain a shift equal to 1565 cm^{-1} , which only deviates -16 cm^{-1} (-0.002 eV) from the supermolecular results. The error, as compared to the supermolecular results, is reduced by a factor of ~ 18 going from the TIP3P to the SPCpol1 potential. Thus, an explicit account of polarization effects is very important. In Table 3,

TABLE 3: Electronic Excitation Energy (E_{ex} , eV) Calculated Using the *adz* Basis Set^a

system	method	E_{ex}	δE_{ex}	ΔE_{ex}
Ac + 2 H ₂ O	CCSD	4.746		0.196 (1581)
	CCSD/MM (TIP3P)	4.781	0.035	0.231 (1863)
	CCSD/MM (SPCpol1)	4.744	-0.002	0.194 (1565)
	CCSD/MM (SPCpol2)	4.740	-0.006	0.190 (1532)
Ac (liquid structure)	CCSD	4.458		-0.092 (-742)
Ac (liquid structure + Gh)	CCSD	4.458		-0.092 (-742)
Ac (vacuum structure)	CCSD	4.550		

^a In the CC/MM calculations, the acetone is treated using CC theory, while the water molecules are treated classically using the model indicated. The term δE_{ex} is the change in the excitation energy as compared to the supermolecular calculation (excluding the dielectric continuum). Furthermore, the term ΔE_{ex} is the shift in the excitation energy as compared to the vacuum result (4.550 eV). The numbers in parentheses are the shifts in units of cm^{-1} . In the calculations indicated with Gh, we keep only the basis set of the water molecule.

**Figure 1.** Definitions of the labels used for the acetone molecule.**Figure 2.** Geometry of the B3LYP/atz optimized complex of acetone and two water molecules including the PCM model.

we have also included CC/MM results using the SPCpol2 water potential⁵⁰ (see Table 4). This potential is derived from ab initio CCSD/aug-cc-pVQZ calculations of the dipole moment (and thereby the partial charges) and the dipole polarizability. The difference between the SPCpol1 and SPCpol2 potentials is that the former leads to slightly more compact structures. From Table 3, we find that the SPCpol1 and SPCpol2 potentials essentially give the same results and both set of results are in very good agreement with the supermolecular predictions. In the rest of this paper, we will only consider the simple point-charge (SPC) and SPCpol1 potentials, and we will hereafter refer to the SPCpol1 potential simply as SPCpol.

The conclusion to be drawn from the study of the microsolvated structures is that including explicit polarization effects in the CC/MM potential essentially leads to a reproduction of the supermolecular results for the acetone $n \rightarrow \pi^*$ transition. From a computational point of view, we note that, already in the case of introducing two water molecules, the CPU time is reduced by a factor of ~ 12 when introducing the CC/MM partitioning. Also, the CC/MM method naturally avoids any problems related to BSSE. The very good agreement between

the supermolecular and CC/MM predictions also indicates that, in this case, the effect of introducing dispersion and short-range repulsion interactions directly into the optimization of the CC/MM wave function is expected to be of minor importance.

The predictions based on microsolvated acetone calculations are in very good agreement with the experimental results (1500–1600 cm^{-1} ^{22–24}). The success of the supermolecular predictions in this case, however, cannot be expected to be general and is likely to be due to the use of a small number of solvent molecules in combination with energy-minimized structures. However, this is not consistent with a real liquid.

C. Construction of MD Potentials. Having discussed the results for acetone microsolvated by water, we now turn our attention to much larger samples; e.g., we consider the case of acetone in liquid water. Because of the large number of molecules included in the supersystem in this case, supermolecular ab initio approaches are impossible and semiempirical or effective models must be used. Here, we rely on the latter approach, i.e., we consider the CC/MM model with solute–solvent configurations based upon MD simulations.

The molecular geometry of acetone together with the parameters used in the simulations are shown in Tables 2 and 4, respectively. The molecular geometry of acetone in a vacuum has been obtained by performing a geometry optimization at the B3LYP/aug-cc-pVTZ level of theory (Figure 1). As seen from Table 2, the vacuum geometry compares well with the available experimental data, although the CO bond length is slightly underestimated (0.005 Å). For the geometry of acetone in water, we include in the geometry optimization explicitly two water molecules together with a polarizable continuum model (PCM)⁵¹ description of the bulk. Table 2 illustrates that the main effect of the solvent is a lengthening of the CO bond and a shortening of the CC bonds. In the MD simulations, we use the “in water” geometry, whereas the “in vacuum” geometry is used as the vacuum reference in the calculation of the shift in the $n \rightarrow \pi^*$ electronic excitation energy (including geometrical distortions). All geometry optimizations have been performed using the *Gaussian 03* program.⁴⁷ We note that the introduction of the two water molecules reduces the symmetry of the (super)system (see Figure 2). However, since two such equivalent configurations may be derived, we simply averaged over these two and thereby obtain the desired C_{2v} symmetry of acetone in the liquid state. It is also possible to constrain the symmetry to be C_{2v} (including the two water molecules). However, in this case, we always find at least one imaginary frequency and thereby not a true energy minimum. The partial charges have been derived using the CHelpG procedure⁵² as implemented in *Gaussian 03* (B3LYP/aug-cc-pVTZ). Furthermore, we constrain the dipole moment to the ab initio value. For the construction of the SPC potential, we also include the PCM in the calculation of the charges in order to introduce the

TABLE 4: Parameters Used in the MD Simulations^a

molecule	model	atom	charge	polarizability (\AA^3)	σ (\AA)	ϵ (kcal/mol)
(CH ₃) ₂ CO	SPC	O	-0.6582		2.960	0.210
		C1	0.7600		3.750	0.105
		C2	-0.3706		3.910	0.160
		H1	0.1033		0.000	0.000
		H2	0.1082		0.000	0.000
(CH ₃) ₂ CO	SPCpol	O	-0.5604	0.000 0.000 0.000	2.960	0.210
		C1	0.7044	6.879 5.082 7.025	3.750	0.105
		C2	-0.3461	0.000 0.000 0.000	3.910	0.160
		H1	0.1021	0.000 0.000 0.000	0.000	0.000
		H2	0.0860	0.000 0.000 0.000	0.000	0.000
H ₂ O	TIP3P	O	-0.8340		3.1507	0.1521
		H	0.4170		0.000	0.000
H ₂ O	SPCpol1	O	-0.6690	1.440 1.440 1.440	3.1660	0.1555
		H	0.3345	0.000 0.000 0.000	0.000	0.000
H ₂ O	SPCpol2	O	-0.6620	1.408 1.408 1.408	3.1660	0.1555
		H	0.3310	0.000 0.000 0.000	0.000	0.000

^aThe components of the polarizability tensor are written according to $(\alpha_{xx}, \alpha_{yy}, \alpha_{zz})$. The σ 's and ϵ 's are the OPLS parameters from ref 58.

effect (although implicitly) of the solvent into the charges. This leads to enhanced charges as compared to the vacuum case. In principle, it would also be possible to introduce explicit water molecules in such calculation. Investigations along this line, however, always lead to total charges different from zero on acetone, which of course is not desirable.

For the SPCpol potential, we use the charges obtained without the PCM and include instead a dipole polarizability tensor (B3LYP/aug-cc-pVTZ) in order to account for explicit polarization effects. We note that the calculated polarizability tensor compares well with the experimental results⁵³ (7.15, 5.16, and 7.05 \AA^3 for the xx , yy , and zz components, respectively). In the simulation, the dipole polarizability tensor is placed at the carbonyl carbon. As seen in Table 4, the main difference between the two potentials is the reduced magnitude of the charges at the chromophore in the SPCpol potential as compared to the SPC potential.

For the description of the water molecules, we use the TIP3P water model,⁴⁸ which belongs to the class of SPC models as well as the SPCpol water model.⁴⁹ The latter includes explicit polarization. The parameters for these two water models are listed in Table 4.

Our emphasis is on the shift in the $n \rightarrow \pi^*$ electronic excitation energy going from vacuum to water solution. As discussed already, the main effect on the acetone geometry due to the solvent is (i) lengthening of the CO bond ($\sim 1.24\%$) and (ii) shortening of the CC bonds ($\sim -0.66\%$). Actually, the lengthening of the CO bond has a significant effect on the $n \rightarrow \pi^*$ electronic excitation energy. In Figure 3, we show the $n \rightarrow \pi^*$ electronic excitation energy as a function of the CO bond length. The value of 1.210 \AA is equivalent to the vacuum case, and the result at 1.225 \AA corresponds to the CO bond length found in the water solution. As seen from this figure, the excitation energy decreases around 2.1% ($\sim 800 \text{ cm}^{-1}$) upon enlarging the CO bond length. Thus, geometrical effects are in this case significant and should be included in the calculation of the shift in the $n \rightarrow \pi^*$ electronic excitation energy. Actually, increasing the CO bond length with 0.005 \AA , i.e., to the bond length found experimentally, and including the effects of triples excitations (CC3), we find corrections to the $n \rightarrow \pi^*$ electronic excitation energy of -255 cm^{-1} (geometry) and -218 cm^{-1} (triples excitations) leading to a best estimate for the electronic excitation energy of 4.491 eV, which compares excellently with the experimental gas-phase results (4.488 eV).

D. The MD Simulations. The MD simulations have been performed with the MOLSIM⁵⁴ program package. We consider

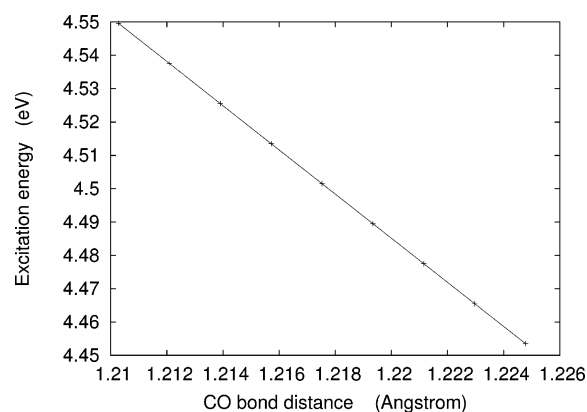


Figure 3. The $n \rightarrow \pi^*$ electronic excitation energy as a function of the CO bond length. Results refer to CCSD/adz.

a cubic box containing 511 rigid water molecules and 1 rigid acetone molecule at the temperature of 298.15 K. Periodic boundary conditions were used, and the time step was 2 fs. A spherical cutoff distance at one-half the box length was used to truncate the intermolecular interactions. Furthermore, a reaction field description was used in order to include long-range interactions.^{55,56} The equilibration was carried out for 600 ps. Next, the production run was performed for 600 000 time steps (1.2 ns), and configurations were dumped every 500 time step (every 1 ps). Thus, we have a total of 1200 configurations to be considered in the mixed quantum-classical calculations. The length of the cubic box was determined using the experimental liquid density for water⁵⁷ ($\rho_{298.15} = 997.0470 \text{ kg/m}^3$).

As in the case of microsolvation, we consider two intermolecular force fields differing in the way polarization is accounted for. Thus, the SPC potential includes van der Waals dispersion and repulsion parameters together with a Coulomb potential, and the SPCpol potential includes, in addition, explicit molecular polarizabilities. The set of dispersion and repulsion parameters are modeled the same way in the SPC and SPCpol potentials, i.e., we use a 6-12-type Lennard-Jones potential

$$V_{\text{LJ}} = \sum_{ij} 4\epsilon_{ij} \left[\left(\frac{\sigma_{ij}}{R_{ij}} \right)^{12} - \left(\frac{\sigma_{ij}}{R_{ij}} \right)^6 \right] \quad (1)$$

where i and j belong to different molecules. Furthermore, for the parameters ϵ_{ij} and σ_{ij} , we use the Lorentz-Berthelot mixing rules, i.e., $\epsilon_{ij} = (\epsilon_i \epsilon_j)^{1/2}$ and $\sigma_{ij} = (\sigma_i + \sigma_j)/2$, where ϵ_i and σ_i are atomic parameters³ taken from ref 58.

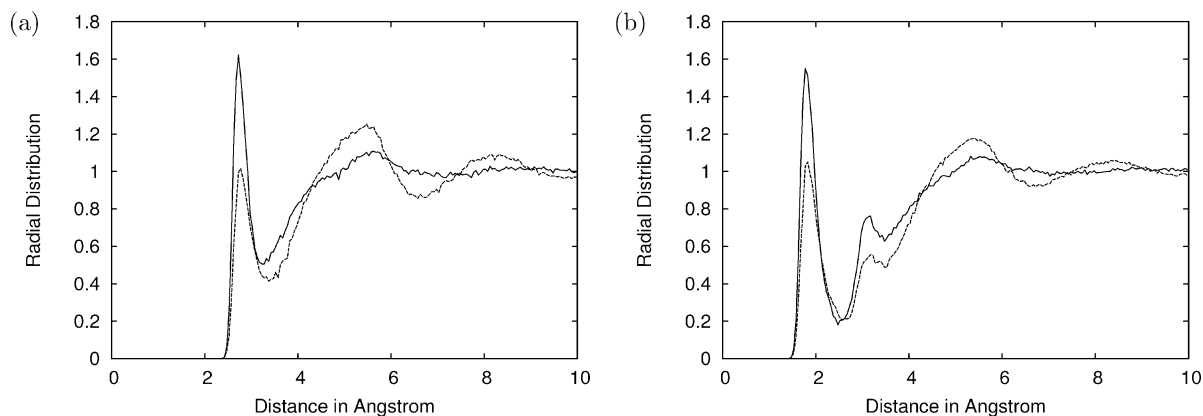


Figure 4. The O((CH₃)₂CO)–O(H₂O) (a) and the O((CH₃)₂CO)–H(H₂O) (b) radial distribution functions. (—): SPC((CH₃)₂CO), TIP3P(H₂O) potentials. (---): SPCpol((CH₃)₂CO), SPCpol(H₂O) potentials.

E. Structural Results Based on the MD Simulations. In Figure 4, we show the radial distribution functions (RDFs) for the carbonyl oxygen and the water oxygen (a) or the water hydrogen (b). In both cases, we show the results from the simulation employing the SPC potentials (solid line) or the SPCpol potentials (broken line).

In the SPC case, a hydrogen bond peak starts around 1.45 Å in the O–H RDF and around 2.40 Å in the O–O RDF. The first maximums in the RDFs are at 1.78 Å (O–H) and 2.75 Å (O–O). This hydrogen bond ends at the first minimum in the RDFs, which is around 2.50 Å in the O–H RDF and around 3.30 Å in the O–O RDF. In the O–H RDF, a clear second maximum is found at 3.16 Å. Thus, in the SPC case, a hydrogen bond length of about 1.78 Å is found. Furthermore, using the intramolecular geometry of the water molecules, we find that this hydrogen bond is almost linear in the carbonyl oxygen–water hydrogen–water oxygen atoms. Spherical integration of the first peak in the O–O RDF gives a coordination number of 2.39. These findings are very similar to the results reported by Coutinho et al.³⁴

In the SPCpol case, the first hydrogen bond also starts at 1.45 Å in the O–H RDF and around 2.45 Å in the O–O RDF. This is similar to the SPC results. The first maxima in the RDFs are at 1.82 Å (O–H) and 2.78 Å (O–O). This hydrogen bond ends around 2.62 Å (O–H) and around 3.40 Å in the O–O RDF. Thus, as compared to the SPC case, this hydrogen bond is slightly longer and as seen from the RDFs also less intense. In the O–H RDF, we also find a clear second maximum around 3.20 Å (corresponding to the second water hydrogen). Thus, the hydrogen bond is, as in the SPC case, linear. The main difference between the SPC and SPCpol simulations is thus the reduced intensity of the first hydrogen bond using the latter potential. Furthermore, the solvent structure above the first solvation shell is seen to be much more structured in the SPCpol case, where in addition to the first maximum in the O–O RDF, we also observe a clear second and a more diffuse third maximum. Likewise, we observe clear maxima in the O–H RDF above the ones corresponding to the first solvation shell. The more structured solvent in the SPCpol simulation is a consequence of the explicit inclusion of polarization effects, which leads to an enhanced cooperativity in the hydrogen bonding network. The less intense first maxima in the SPCpol case is presumable because of the reduced magnitude of the partial charges on the chromophore. Integration of the first peak in the SPCpol O–O RDF gives a coordination number of 1.96, which is lower than in the SPC case.

The conclusion from the structural analysis is that the SPC potential leads to more compact and intense structures (at least

for the first solvation shell) as compared to the SPCpol potential. Thus, at this stage, it can already be expected that the blue shift in the SPC case is enhanced as compared to the SPCpol predictions.

We note that the method used to extract the number of hydrogen bonds must be considered to give an upper limit to the coordination number. This happens since it cannot be assured that all nearest-neighbor structures within a distance smaller than the first minimum in the O–O RDF can be considered truly hydrogen bonded. Another method to extract the number of hydrogen bonds would be to consider, in addition, geometrical and energetic criteria.^{59–64} The energetic criteria must be based on two-body interactions in order not to introduce artifacts in the hydrogen bond definition. In the SPCpol simulations, however, a large part of the interaction energy is due to many-body effects, and a direct comparison between the number of hydrogen bonds in the SPC and SPCpol cases cannot be performed. Therefore, we only include in the discussion of hydrogen bonds the results based upon integration of the O–O RDF, since results based upon this definition may be compared directly between different procedures for introducing polarization effects.

F. Combined Coupled Cluster/Molecular Dynamics Results. Having derived and discussed the solute–solvent configurations, we now consider the calculation of the $n \rightarrow \pi^*$ electronic excitation energy using the CC/MM method. The excitation energy is determined as a statistically averaged vertical excitation energy. The difference with respect to the vertical excitation energy in a vacuum calculation defines the shift. As discussed previously, the acetone molecule is placed in the xz plane with the oxygen atom in the origin and the C_2 axis aligned with the molecular z axis. If not stated differently, we always freeze the four lowest canonical orbitals (all of 1s character) of oxygen and carbon. In the CC/MM calculations, we have used a spherical cutoff radius equal to 10 Å. In a previous study of the $n \rightarrow \pi^*$ electronic excitation energy in formaldehyde, this was found to be sufficient.²⁰ This cutoff radius amounts to including 125–148 water molecules in the CC/MM calculations. We begin by determining the minimum number of solute–solvent configurations to be used in order to predict statistically converged results. Hereafter, we present the final (large basis set) calculations of the specific properties.

1. Convergence with respect to the Number of Solute–Solvent Configurations. In Figure 5, we have shown the convergence of the shift in the $n \rightarrow \pi^*$ electronic excitation energy with respect to the number of solute–solvent configurations included in the statistical averaging using either the SPC (a) or the SPCpol (b) potentials. This first set of calculations has been performed

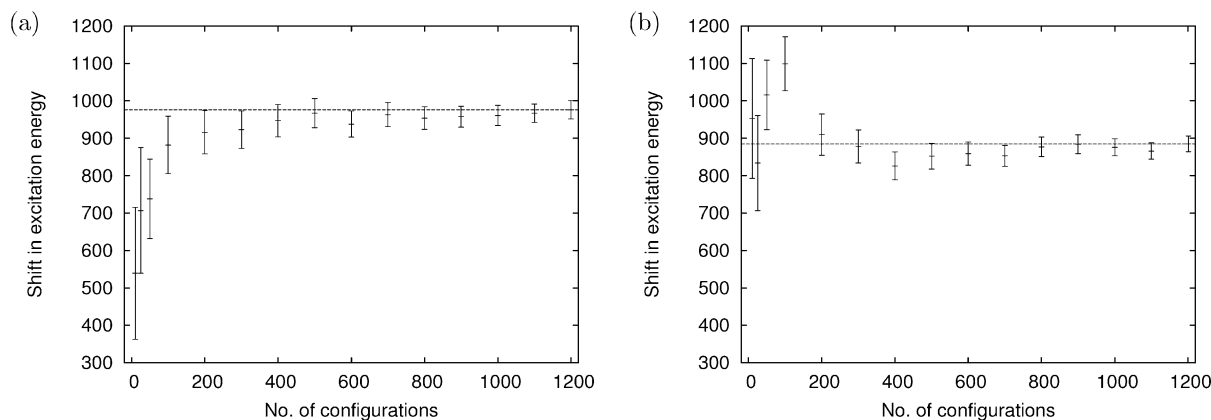


Figure 5. The shift in the $n \rightarrow \pi^*$ electronic excitation energy (in cm^{-1}) as a function of the number of configurations included in the statistical averaging modeling the polarization either implicitly (a) or explicitly (b) obtained by CCSD/6-31++G. The error bars are calculated according to σ/\sqrt{N} . The horizontal line indicates the shift obtained using 1200 solute–solvent configurations. The shifts include the effects of geometrical changes in the molecular structure. The CCSD/6-31++G result for the electronic excitation energy for acetone in a vacuum (employing the vacuum geometry) is 4.4124 eV.

TABLE 5: CCSD Results for the Electronic Excitation Energy (E_{ex} , eV) and the Corresponding Shifts (ΔE_{ex} , cm^{-1}) Calculated Using 1200 Solute–Solvent Configurations and Different MD and/or QM/MM Potentials^a

	SPC/SPC	SPC/SPCpol	SPCpol/SPCpol
E_{ex}	4.533 ± 0.003	4.548 ± 0.003	4.522 ± 0.003
ΔE_{ex}	976 ± 24	1091 ± 24	885 ± 21

^a The nomenclature is MD potential/QM/MM potential. The basis set used is the 6-31++G basis set.

at the CCSD level of theory employing the 6-31++G basis set.⁶⁵ In both cases, we observe significant changes in the property up to around 400 configurations. Including around 800 configurations would represent statistically converged properties, as only small fluctuations in the shift are observed hereafter. Also, using 800 configurations, we find the estimated error in the mean value (σ/\sqrt{N}) to be around 30 cm^{-1} or less. Thus, we include in the final (larger basis set) calculations 800 configurations using either the SPC or SPCpol potential.

At this point, we may comment on the difference in using an explicit or an implicit description of polarization effects. In Table 5, we have collected results (CCSD/6-31++G) for the electronic excitation energy and the corresponding shifts calculated using 1200 solute–solvent configurations from different MD simulations and using different QM/MM potentials. The nomenclature is MD potential/QM/MM potential. From this table, we find a shift of $976 \pm 24 \text{ cm}^{-1}$ using the SPC potential in *both* the MD and CC/MM calculations. Using the SPC potential in the MD simulations but the SPCpol potential in the CC/MM calculations leads to an enhancement of the shift of 115 cm^{-1} . Including, however, the SPCpol potential in *both* the MD and CC/MM calculations predicts a decrease in the shift, as compared to the SPC case, of -91 cm^{-1} . Thus, using SPC-based configurations but the SPCpol potential in the CC/MM calculations leads to a change in the shift in the opposite direction to that observed using the SPCpol potential in *both* the MD and CC/MM calculations. The enhanced value of the shift in the SPC case as compared to the SPCpol case is expected on basis of the RDFs. In section III. D, we found the SPC-based configurations to be more compact, and thereby, the perturbation from the solvent is in this case expected to be more significant.

We note that the use of mixed polarization descriptions (SPC-based configurations combined with SPCpol QM/MM potentials) in connection with predictions of solvent effects on $n \rightarrow$

TABLE 6: Results for the Electronic Excitation Energy (E_{ex} , eV) and the Corresponding Shifts (ΔE_{ex} , cm^{-1}) Together with the Ground- and Excited-State Dipole Moments (μ_z , D)^a

	SPC	SPCpol
E_{ex}	4.700 ± 0.004	4.686 ± 0.003
$\Delta E_{\text{ex}}^{\text{vr}}$	1216 ± 29	1103 ± 26
$\Delta E_{\text{ex}}^{\text{lr}}$	1960 ± 29	1847 ± 26
μ_z^{gs}	4.46 ± 0.01	4.44 ± 0.02
μ_z^{ex}	3.07 ± 0.01	3.01 ± 0.02
${}^n f (\cdot 10^5)$	1.37 ± 0.07	0.97 ± 0.04

^a Also given is the (dimensionless) oscillator strength (in length gauge) for the $n \rightarrow \pi^*$ electronic transition (${}^n f$). For the shift, we include numbers using the vacuum structure as the reference ($E_{\text{ex}}^{\text{vr}}$) together with results obtained using the liquid structure as the "vacuum" reference ($E_{\text{ex}}^{\text{lr}}$). The former include geometrical effects.

π^* electronic transitions for small organic solutes in water has been employed; see, for example, ref 66 (formaldehyde) and ref 67 (acrolein) for recent examples. However, our findings do not support such procedures. The generations of the configurations are usually the least expensive part of the hybrid method. Thus, overall, only slightly more computational time would be needed in order to include polarization explicitly in the MD simulations, whereas a considerable reduction in computational time is achieved using SPC potentials (as compared to SPCpol potentials) in the QM/MM calculations. Thereby, from a computational point of view, the use of mixed polarization descriptions, as already discussed, seems somewhat unbalanced.

2. Large Basis Set Calculations. Having determined both a proper basis set and the number of solute–solvent configurations needed in the statistical analysis, we turn to the large basis set calculations. Thus, in the following, we use the aug-cc-pVDZ basis set in the property calculations together with 800 solute–solvent configurations in the statistical part. In Table 6, we present the results for the electronic excitation energy, the corresponding shifts, the dipole moments, and the (length gauge) oscillator strength. First, we observe that the introduction of explicit polarization effects in both the generation of the solute–solvent configurations and the CC/MM calculations lead to a small decrease in the magnitude of the electronic excitation energy as compared to the SPC potential. However, both predictions are in very good agreement with the experimental result for the liquid phase (4.682 eV). Concerning the corresponding shifts in the electronic excitation energy, we have in

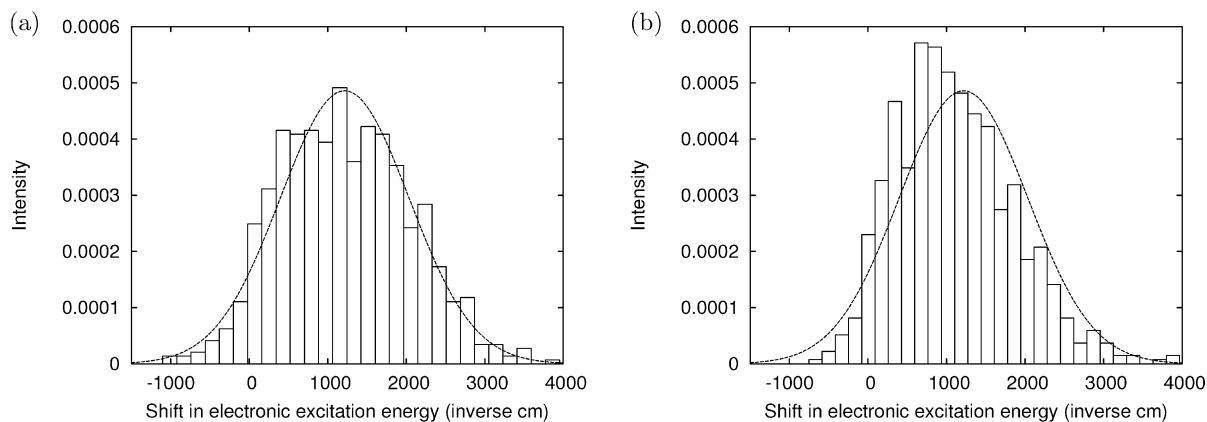


Figure 6. The statistical distribution of the shift in the $n \rightarrow \pi^*$ electronic excitation energy calculated using CCSD/aug-cc-pVDZ and 800 solute-solvent configurations. Polarization effects are treated either implicitly (a) or explicitly (b).

TABLE 7: Summary of Calculated Solvatochromic Shifts (ΔE_{ex}) of $n \rightarrow \pi^*$ Excitation Energy in Acetone Using Different Theoretical Approaches^a

ref	method	basis set	E_{ex}^v (eV)	E_{ex}^l (eV)	ΔE_{ex} (cm^{-1})
Liao et al. ²⁵	supermolecule CASSCF	6-31G**	4.3481	4.6004–4.7479	2035–3225
Ten-no et al. ²⁶	RISM-SCF	DZP	4.013	4.353	2742
Cossi et al. ²⁷	supermolecule CASSCF/PCM	6-31G*	4.612	4.909	2397
Serrano-Andrés et al. ²⁸	CASPT2/DC	ANO 4s3p1d/2s	4.36	4.39	242
	supermolecule CASPT2	ANO 4s3p1d/2s	4.36	4.54	1452
	supermolecule CASPT2/DC	ANO 4s3p1d/2s	4.36	4.50	1129
Aquilante et al. ³³	supermolecule TD-DFT	6-311++G(2d,2p)	4.43	4.71	2258
	supermolecule TD-DFT/PCM	6-311++G(2d,2p)	4.43	4.81	3065
	MD TD-DFT/PCM	6-311++G(2d,2p)	4.43	4.62	1532 \pm 807
Crescenzi et al. ²⁹	supermolecule TD-DFT/PCM	6-311++G(2d,2p)/ 6-31+G(d,p)	4.48	4.86	3065
	CPMD TD-DFT	6-311++G(2d,2p)/ 6-31+G(d,p)	4.28 \pm 0.02	4.49 \pm 0.01	1694
Röhrig et al. ³⁰	CPMD QM/MM ROKS	plane waves	3.85 \pm 0.09	4.10 \pm 0.12	2016
Bernasconi et al. ³¹	CPMD TD-DFT	plane waves	4.18	4.37	1532
Sulpizi et al. ³²	CPMD QM/MM TD-DFT	plane waves	4.22	4.46 \pm 0.15	1936
Coutinho et al. ³⁴	MC INDO/CIS	--	--	--	1310 \pm 40
Coutinho et al. ³⁵	supermolecule CIS	6-311++G*	--	--	1530
	MC CIS	6-311++G*	--	--	1150 \pm 120
Grozema et al. ²¹	MC QM/MM HF	DZP	3.725	3.910	1493 \pm 514
Gao ³⁶	MC AM1-CI/MM	--	--	--	1694 \pm 84
present work	supermolecule CCSD	aug-cc-pVDZ	4.550(4.491 ^b)	4.746	1581
	MD QM/MM(SPC) CCSD	aug-cc-pVDZ	4.550(4.491 ^b)	4.700 \pm 0.004	1216 \pm 29
	MD QM/MM(SPCpol) CCSD	aug-cc-pVDZ	4.550(4.491 ^b)	4.686 \pm 0.003	1103 \pm 26
experiment ^{22–24}			4.488	4.682	1500–1600

^a Also shown is the absolute magnitude of the excitation energies in vacuum (E_{ex}^v) as well as in solvent (E_{ex}^l). ^b With triples and geometrical corrections; see section III. C.

Table 6 given results both including ($E_{\text{ex}}^{\text{vr}}$) and excluding ($E_{\text{ex}}^{\text{lr}}$) geometrical effects, i.e., in the latter approach, we use the liquid-phase geometry of acetone as the vacuum reference. Here, we find that the geometrical effects reduce the shift by 744 cm^{-1} and may thus be considered very important. For the dipole moments, we find for both the ground and excited states a significant increase when going to the liquid phase. For the ground state, the increase is around 1.5 D, and for the excited state, the increase is approximately 1.4 D. This is true using either the SPC or the SPCpol potentials. We note that in the SPC MD simulation the acetone molecule has a (classical) permanent dipole moment equal to 4.19 D, which is in reasonable agreement with the SPC CC/MM results in Table 6. The oscillator strengths are very small in both the SPC and SPCpol cases, e.g., around $1 \cdot 10^{-5}$ (dimensionless). This oscillator strength is solely due to direct solvent effects on the electronic structure, e.g., local symmetry reductions due to hydrogen bonding, and contains no contribution due to vibronic coupling. Thus, it is expected that this result is significantly underestimated as compared to experimental results.

Comparing the results for the shift in the electronic excitation energy obtained from the supermolecular and simulation approaches, we find a decrease in the results based upon the MD simulations. This is anticipated to be due to the use of energy-minimized structures in the supermolecular calculations giving larger solvation effects as compared to the simulation results. The supermolecular results are based on only one solute-solvent configuration. However, because of the statistical nature of a liquid, it is expected that a large spread in the property results may be found. In Figure 6, we have shown the distribution of the shift in the electronic excitation energy based upon the configurations from the MD simulations. The absolute frequencies have been converted to relative frequencies and divided by the width of the histogram boxes. Also, we have plotted a Gaussian probability density function where σ (the standard deviation) and μ (the mean value of the property) have been taken from the statistical analysis. Indeed, we find the spread to be very large, e.g., around 5000 cm^{-1} using either the SPC or the SPCpol potentials. Also, we observe that few solute-solvent configurations possess a small red shift in the electronic

excitation energy. Obviously, a proper averaging over different solute–solvent configurations is mandatory.

Compared to the experimental results for the shift in the electronic excitation energy (1500–1600 cm^{-1}), we obtain in the simulation-based approach a somewhat underestimated result. As discussed previously, the electronic excitation energy is extremely dependent on the CO bond length. In the determination of the liquid structure, we used geometry optimizations of acetone plus two explicit water molecules together with the PCM. It is possible that, because of the use of energy-minimized configurations, solvent effects are overestimated in such approaches. Thereby, it is possible that the liquid structure of acetone suffers from an overly significant lengthening of the CO bond. This will, according to Figure 3, lead to an underestimation of the shift in the $n \rightarrow \pi^*$ electronic transition. Also, we note that shifting the CO bond length in acetone in a vacuum to the experimental value would lead to an enhanced shift of around 255 cm^{-1} . This aspect is likely the most significant source of uncertainty in our predictions.

3. Comparison with Other Theoretical Approaches. Table 7 collects some previously reported results for the computed gas phase–aqueous solution shifts of the $n \rightarrow \pi^*$ excitation energy in acetone. The predicted numbers possess a large spread, i.e., from ~ 1100 up to 3200 cm^{-1} . Our results have found their place at the lower end of the list. The broad range of predicted shifts also impresses on us the significance of using an accurate geometry of the molecular system involved in the calculation of excitation energies. Note that some authors^{27,28} have considered the C_{2v} geometries of acetone–water complexes. However, we have found this to possess at least one imaginary vibrational frequency. In some of the investigations,^{21,25,27} the excitation energies were calculated using basis sets without diffuse functions. From our point of view, diffuse functions in the basis set are mandatory when considering intermolecular interactions and excitation energies. In general, the shifts predicted by supermolecular calculations are greater in magnitude than those from MD or MC simulations. This is in accordance with the assumption that the consideration of equilibrium structures containing one acetone and a few water molecules overestimates the solvent effects. Also, we note that in some of the investigations which predict rather good results for the shift in excitation energy, the absolute value is predicted quite poorly as compared to experimental data (see, for example, refs 21, 28–31).

IV. Summary

In this work, we have studied the gas-to-aqueous-solution shift of $n \rightarrow \pi^*$ excitation energy in acetone. A combined coupled cluster/molecular mechanics electronic structure theory method was used for this purpose. Basis set analysis revealed that the aug-cc-pVDZ basis set is accurate enough to predict the excitation energy of the $n \rightarrow \pi^*$ transition in acetone. Considering a supermolecular system of one acetone and two water molecules, we obtained a shift in the excitation energy compared to vacuum of 1581 cm^{-1} . It was also found that in this case the explicit account of polarization effects in the CC/MM potential is mandatory when considering the excitation energies. The good agreement of excitation energies calculated at CC and CC/MM levels of theory suggests that the effects of dispersion and short-range repulsion are not significant in this case. A sufficient number of configurations, i.e., 800, were determined by CCSD/MM calculation with the fairly small 6-31++G basis set to provide statistically converged results for the excitation energy.

The large basis set calculation yielded accurate values of $n \rightarrow \pi^*$ excitation energy in acetone in the gas phase as well as in the liquid phase. However, the reproduced shifts of $1216 \pm 29 \text{ cm}^{-1}$ (SPC) and $1103 \pm 26 \text{ cm}^{-1}$ (SPCpol) are slightly underestimated as compared to experimental data indicating a shift of 1500–1600 cm^{-1} . The better agreement between the supermolecular calculations and experimental results is probably fortuitous. In any way, we find that proper statistical averaging is mandatory, and such averaging should also be considered for supermolecular calculations before a rigorous comparison with experimental data is performed. We note that the experimental determination of the shift in the electronic excitation energy is based on the identification of the theoretical vertical electronic excitation energies with the position of maximum absorption in the experimental spectrum. This, however, is of course only approximate. For the case of acetone, an additional uncertainty in this identification is introduced because of a vibronic contribution to the absorption intensity. With these reservations in mind, the calculated results compare fairly well with the experimental data.

Geometrical effects, e.g., the length of the CO bond, are found to influence the excitation energy to a great extent. Thereby, an accurate geometry of acetone used in the MD simulations is of great importance. The explicit consideration of polarization is found to slightly lower the excitation energy and should be included in both the MD simulation and the QM/MM calculation of the excitation energy. A large spread in excitation energies calculated using configurations from MD simulation was observed, emphasizing the importance of an adequate number of configurations necessary to reproduce reliable statistically converged results for the excitation energy.

Acknowledgment. O.C. acknowledges support from the Danish Research Agency (FNU), Danish National Research Foundation, and Danish Center for Scientific Computing (DCSC). K.V.M. thanks FNU, Statens Teknisk Videnskabelige Forskningsråd, DCSC, and the EU networks MOLPROP, NANOQUANT, and THEONET II for support. J.K. acknowledges Prof. Sylvio Canuto (University of São Paulo) for stimulating discussions on the subject of solvation and Prof. Per Linse (University of Lund) for advice concerning MOLSIM. K.A. acknowledges the EU Socrates – Erasmus program for support and the quantum chemistry group at the University of Copenhagen for a warm welcome.

References and Notes

- (1) Böttcher, C. *Theory of electronic polarization*; Elsevier Scientific: Amsterdam, 1973.
- (2) Tomasi, J.; Persico, M. *Chem. Rev.* **1994**, *94*, 2027.
- (3) Allen, M. P.; Tildesley, D. J. *Computer Simulation of Liquids*; Clarendon Press: Oxford, 1987.
- (4) Car, R.; Parrinello, M. *Phys. Rev. Lett.* **1985**, *55*, 2471.
- (5) Thompson, M. A. *J. Phys. Chem.* **1996**, *100*, 14492.
- (6) Warshel, A.; Levitt, M. *J. Mol. Biol.* **1976**, *103*, 227.
- (7) Singh, U. C.; Kollman, P. A. *J. Comput. Chem.* **1986**, *7*, 718.
- (8) Field, M. J.; Bash, P. A.; Karplus, M. *J. Comput. Chem.* **1990**, *11*, 700.
- (9) Chalmet, S.; Rinaldi, D.; Ruiz-López, M. F. *Int. J. Quantum Chem.* **2001**, *84*, 559.
- (10) Moriarty, N. W.; Karlström, G. *J. Chem. Phys.* **1997**, *106*, 6470.
- (11) Warshel, A. *J. Phys. Chem.* **1979**, *83*, 1640.
- (12) Luzhkov, V.; Warshel, A. *J. Am. Chem. Soc.* **1991**, *113*, 4491.
- (13) Gao, J.; Byun, K. *Theor. Chem. Acc.* **1997**, *96*, 151.
- (14) Thompson, M. A.; Schenter, G. K. *J. Phys. Chem.* **1995**, *99*, 6374.
- (15) Warshel, A.; Chu, Z. T. *J. Phys. Chem. B* **2001**, *105*, 9857.
- (16) Kongsted, J.; Osted, A.; Mikkelsen, K. V.; Christiansen, O. *Mol. Phys.* **2002**, *100*, 1813.
- (17) Kongsted, J.; Osted, A.; Mikkelsen, K. V.; Christiansen, O. *J. Chem. Phys.* **2002**, *118*, 1620.
- (18) Kongsted, J.; Osted, A.; Mikkelsen, K. V.; Christiansen, O. *J. Chem. Phys.* **2003**, *119*, 10519.

- (19) Kongsted, J.; Osted, A.; Mikkelsen, K. V.; Christiansen, O. *J. Chem. Phys.* **2004**, *120*, 3787.
- (20) Kongsted, J.; Osted, A.; Mikkelsen, K. V.; Åstrand, P. O.; Christiansen, O. *J. Chem. Phys.* **2004**, *121*, 8435.
- (21) Grozema, F. C.; van Duijnen, P. Th. *J. Phys. Chem. A* **1998**, *102*, 7984.
- (22) Hayes, W. P.; Timmons, C. J. *Spectrochim. Acta* **1965**, *21*, 529.
- (23) Bayliss, N. S.; Wills-Johnson, G. *Spectrochim. Acta, Part A* **1968**, *24*, 551.
- (24) Bayliss, N. S.; McRae, E. G. *J. Phys. Chem.* **1954**, *58*, 1006.
- (25) Liao, D. W.; Mebel, A. M.; Chen, Y. T.; Lin, S. H. *J. Phys. Chem. A* **1997**, *101*, 9925.
- (26) Ten-no, S.; Hirata, F.; Kato, S. *J. Chem. Phys.* **1994**, *100*, 7443.
- (27) Cossi, M.; Barone, V. *J. Chem. Phys.* **2000**, *112*, 2427.
- (28) Serrano-Andrés, L.; Fülischer, M. P.; Karlström, G. *Int. J. Quantum Chem.* **1997**, *65*, 167.
- (29) Crescenzi, O.; Pavone, M.; De Angelis, F.; Barone, V. *J. Phys. Chem. B* **2005**, *109*, 445.
- (30) Röhrig, U. F.; Frank, I.; Hutter, J.; Laio, A.; VandeVondele, J.; Rothlisberger, U. *ChemPhysChem* **2003**, *4*, 1177.
- (31) Bernasconi, L.; Sprik, M.; Hutter, J. *J. Chem. Phys.* **2003**, *119*, 12417.
- (32) Sulpizi, M.; Röhrig, U. F.; Hutter, J.; Rothlisberger, U. *Int. J. Quantum Chem.* **2005**, *101*, 671.
- (33) Aquilante, F.; Cossi, M.; Crescenzi, O.; Scalmani, G.; Barone, V. *Mol. Phys.* **2003**, *101*, 1945.
- (34) Coutinho, K.; Canuto, S. *THEOCHEM* **2003**, *632*, 235.
- (35) Coutinho, K.; Saavedra, N.; Canuto, S. *THEOCHEM* **1999**, *466*, 69.
- (36) Gao, J. *J. Am. Chem. Soc.* **1994**, *116*, 9324.
- (37) Gwaltney, S. R.; Bartlett, R. J. *Chem. Phys. Lett.* **1995**, *241*, 26.
- (38) Christiansen, O.; Jørgensen, P.; Hättig, C. *Int. J. Quantum Chem.* **1998**, *68*, 1.
- (39) Kongsted, J.; Osted, A.; Mikkelsen, K. V.; Christiansen, O. *J. Phys. Chem. A* **2003**, *107*, 2578.
- (40) Olsen, J.; Jørgensen, P. *J. Chem. Phys.* **1985**, *82*, 3235.
- (41) Helgaker, T.; Jensen, H. J. Aa.; Jørgensen, P.; Olsen, J.; Ruud, K.; Ågren, H.; Auer, A. A.; Bak, K. L.; Bakken, V.; Christiansen, O.; Coriani, S.; Dahle, P.; Dalskov, E. K.; Enevoldsen, T.; Fernandez, B.; Hättig, C.; Hald, K.; Halkier, A.; Heiberg, H.; Hetttema, H.; Jonsson, D.; Kirpekar, S.; Kobayashi, R.; Koch, H.; Mikkelsen, K. V.; Norman, P.; Packer, M. J.; Pedersen, T. B.; Ruden, T. A.; Sanchez, A.; Saue, T.; Sauer, S. P. A.; Schimmelpfennig, B.; Sylvester-Hvid, K. O.; Taylor, P. R.; Vahtras, O. Dalton, an ab initio electronic structure program, release 1.2; 2001. See <http://www.kjemi.uio.no/software/dalton/dalton.html>
- (42) Purvis, G. D.; Bartlett, R. J. *J. Chem. Phys.* **1982**, *76*, 1910.
- (43) Christiansen, O. MidasCpp, Molecular Interactions and Simulation in c++ Chemistry Program Package; 2004. See <http://www.chem.au.dk/~ove/>
- (44) Kendall, R. A.; Dunning, T. H.; Harrison, R. J. *J. Chem. Phys.* **1992**, *96*, 6796.
- (45) Woon, D. E.; Dunning, T. H. *J. Chem. Phys.* **1994**, *100*, 2975.
- (46) Christiansen, O.; Koch, H.; Jørgensen, P. *J. Chem. Phys.* **1995**, *103*, 7429.
- (47) Frisch, M. J.; Trucks, G. W.; Schlegel, H. B.; Scuseria, G. E.; Robb, M. A.; Cheeseman, J. R.; Montgomery, J. A., Jr.; Vreven, T.; Kudin, K. N.; Burant, J. C.; Millam, J. M.; Iyengar, S. S.; Tomasi, J.; Barone, V.; Mennucci, B.; Cossi, M.; Scalmani, G.; Rega, N.; Petersson, G. A.; Nakatsuji, H.; Hada, M.; Ehara, M.; Toyota, K.; Fukuda, R.; Hasegawa, J.; Ishida, M.; Nakajima, T.; Honda, Y.; Kitao, O.; Nakai, H.; Klene, M.; Li, X.; Knox, J. E.; Hratchian, H. P.; Cross, J. B.; Bakken, V.; Adamo, C.; Jaramillo, J.; Gomperts, R.; Stratmann, R. E.; Yazyev, O.; Austin, A. J.; Cammi, R.; Pomelli, C.; Ochterski, J. W.; Ayala, P. Y.; Morokuma, K.; Voth, G. A.; Salvador, P.; Dannenberg, J. J.; Zakrzewski, V. G.; Dapprich, S.; Daniels, A. D.; Strain, M. C.; Farkas, O.; Malick, D. K.; Rabuck, A. D.; Raghavachari, K.; Foresman, J. B.; Ortiz, J. V.; Cui, Q.; Baboul, A. G.; Clifford, S.; Cioslowski, J.; Stefanov, B. B.; Liu, G.; Liashenko, A.; Piskorz, P.; Komaromi, I.; Martin, R. L.; Fox, D. J.; Keith, T.; Al-Laham, M. A.; Peng, C. Y.; Nanayakkara, A.; Challacombe, M.; Gill, P. M. W.; Johnson, B.; Chen, W.; Wong, M. W.; Gonzalez, C.; Pople, J. A. *Gaussian 03*, revision B.05; Gaussian, Inc.: Wallingford, CT, 2004.
- (48) Jørgensen, W. L. *J. Am. Chem. Soc.* **1981**, *103*, 335.
- (49) Ahlström, P.; Wallqvist, A.; Engström, S.; Jönsson, B. *Mol. Phys.* **1989**, *68*, 563.
- (50) Kongsted, J.; Osted, A.; Pedersen, T. B.; Mikkelsen, K. V.; Christiansen, O. *J. Phys. Chem. A* **2004**, *108*, 8646.
- (51) Miertuš, S.; Scrocco, E.; Tomasi, J. *Chem. Phys.* **1981**, *55*, 117.
- (52) Breneman, C. M.; Wiberg, K. B. *J. Comput. Chem.* **1990**, *11*, 361.
- (53) Burnham, A. K.; Gierke, T. D. *J. Chem. Phys.* **1980**, *73*, 4822.
- (54) Linse, P. (University of Lund, Sweden) MOLSIM, an integrated md/mc/bd simulation program belonging to the MOLSIM package, version 3.3.0; 2001.
- (55) Nymand, T. M.; Linse, P. *J. Chem. Phys.* **2000**, *112*, 6386.
- (56) Nymand, T. M.; Linse, P. *J. Chem. Phys.* **2000**, *112*, 6152.
- (57) Tanaka, M.; Girard, G.; Davis, R.; Peuto, A.; Bignell, N. *Metrologia* **2001**, *38*, 301.
- (58) Jørgensen, W. L.; Briggs, J. M.; Contreras, M. L. *J. Phys. Chem.* **1990**, *94*, 1683.
- (59) Rahman, A.; Stlinger, F. H. *J. Chem. Phys.* **1971**, *55*, 3336.
- (60) Stlinger, F. H.; Rahman, A. *J. Chem. Phys.* **1974**, *60*, 1545.
- (61) Stlinger, F. H. *Adv. Chem. Phys.* **1975**, *31*, 1.
- (62) Mezei, M.; Beveridge, D. L. *J. Chem. Phys.* **1981**, *74*, 622.
- (63) Malaspina, T.; Coutinho, K.; Canuto, S. *J. Chem. Phys.* **2002**, *117*, 1692.
- (64) Jørgensen, W. L.; Chandrasekhar, J. D.; Madura, J.; Impey, R. W.; Klein, M. L. *J. Chem. Phys.* **1983**, *79*, 926.
- (65) Frisch, M. J.; Pople, J. A.; Binkley, J. S. *J. Chem. Phys.* **1984**, *80*, 3265.
- (66) Kawashima, Y.; Dupuis, M.; Hirao, K. *J. Chem. Phys.* **2002**, *117*, 248.
- (67) Martín, M. E.; Losa, A. M.; Fdez.-Galván, I.; Aguilar, M. A. *J. Chem. Phys.* **2004**, *121*, 3710.
- (68) Sverdlov, L. M.; Kovner, M. A.; Krainov, E. P. *Vibrational Spectra of Polyatomic Molecules*; Wiley: New York, 1974.